Raman and Infrared Spectra, Conformational Stability, Normal Coordinate Analysis, Vibrational Assignment, and ab Initio Calculations of 3,3-Difluorobutene

Gamil A. Guirgis,† Xiaodong Zhu,‡ Zhenhong Yu, and James R. Durig*

Department of Chemistry, University of Missouri—Kansas City, Kansas City, Missouri 64110-2499

Received: September 24, 1999; In Final Form: February 15, 2000

The Raman spectra (3300−10 cm^{-1}) of gaseous, liquid, and solid 3,3-difluorobutene, $CH_2CHCF_2CH_3$, and the infrared spectra (3400−60 cm^{-1}) of the gas, xenon solution, and solid have been recorded. The spectra of the fluid phases are consistent with two stable conformers in equilibrium at ambient temperature. Utilizing two conformer pairs from the mid-infrared spectra of the xenon solution as a function of temperature (−100 to −55 °C), the enthalpy difference has been determined to be 68 ± 4 cm^{-1} (0.81 ± 0.05 kJ/mol) where the cis conformer, where the CH_3 group is cis to the double bond, is the more stable form. These spectral data indicate that the cis conformer is more stable than the gauche form in both the gaseous and liquid phases, but it is possible to obtain *either* conformer in the solid. The fundamental asymmetric torsion for the gauche conformer was observed at 84.27 cm^{-1}, and the overtone of the corresponding mode for the cis conformer was observed at 150.37 cm^{-1}. The potential function governing the conformer interconversion has been obtained and the constants are $V_1 = 284 \pm 15$, $V_2 = -164 \pm 13$, $V_3 = 632 \pm 7$, $V_4 = -30 \pm 5$, $V_6 = -39 \pm 3$. The gauche to cis barrier is 489 cm^{-1} (5.85 kJ/mol) and the gauche to gauche barrier is 848 cm^{-1} (10.14 kJ/mol). Vibrational assignments for the 30 normal modes for both the cis and gauche conformers are proposed. The structural parameters, dipole moments, conformational stability, vibrational frequencies, infrared intensities, and Raman activities have been determined from ab initio calculations. The predicted conformational stability at all levels of calculation up to MP2/6-311+G(2d,2p) is *not* consistent with the experimental results. These experimental and theoretical results are compared to the corresponding quantities of some similar molecules.

Introduction

Since 1-butene is the simplest alkene which exists as an equilibrium mixture of high- and low-energy rotational isomers, it has been the subject of many spectroscopic and theoretical studies to determine the energy difference between the two stable conformers, i.e., the cis and gauche forms, where the methyl group lies, respectively, eclipsing the double bond or skewed from this position by about 120°. Previous techniques used to determine the structures and relative stability of the different conformers of 1-butene have been vibrational spectroscopy,[1−4] nuclear magnetic resonance spectroscopy,[5−8] and microwave spectroscopy.[9] The studies carried out by using NMR[5−8] and vibrational spectroscopy[1−4] gave results which indicated that the cis conformer is more stable, whereas the analysis of the microwave spectrum[9] led to the opposite conclusion. Nevertheless, the most recent vibrational study[3] clearly shows that the cis conformer is the more stable form in the gas.

It has been found that methyl barriers for some fluorine-substituted hydrocarbons have values similar to the corresponding hydrocarbon[10−12] and, therefore, one would predict the 3,3-difluorobutene molecule to have two conformers whose energy difference is similar to that of 1-butene. Additionally, the potential function governing the conformer interconversion of 3,3-difluorobutene could also be similar to that of 1-butene. Thus, as a continuation of our studies of substituted butene molecules,[13−17] the determination of the conformational stability for 3,3-difluorobutene has been carried out by an investigation of the temperature-dependent FT-IR spectra in xenon solutions along with the ab initio calculations. Additionally, we have recorded the infrared and Raman spectra of the fluid and solid phases. The conformational stability, optimized geometry, force constants, vibrational frequencies, infrared intensity, Raman activities, and depolarization ratios have been obtained from ab initio RHF (restricted Hartree−Fock) and/or with full electron correlation by the perturbation method to the second-order (MP2) calculations for comparison with the experimental quantities when appropriate. The results of this vibrational spectroscopic and theoretical study are reported herein.

Experimental Section

The sample of 3,3-difluorobutene was provided by Bayer Corp., Charleston, SC. The sample was purified by using a low-temperature, low-pressure fractionation column and the sample was stored at low temperature under vacuum until used. The purity of the sample was checked by comparing the mid-infrared spectrum with that predicted from the ab initio calculations and mass spectral analysis. All sample transfers were carried out under vacuum to avoid contamination.

The Raman spectra of gaseous, liquid, and solid 3,3-difluorobutene from 3200 to 20 cm^{-1} were recorded on a Cary model 82 spectrometer equipped with a Spectra-Physics model 171 argon ion laser operating on the 5145 Å line. Laser power at the sample ranged from 0.4 to 2.0 W depending on the physical state of the sample. The spectrum of the gas was recorded using a standard Cary multipass accessory. The spectrum of the liquid was obtained from the sample sealed in

* Corresponding author. Phone: 01 816-235-1136. Fax: 01 816-235-5191. E-mail: durigj@umkc.edu.

† Permanent address: Analytical R/D Department, Organic Products Division, Bayer Corp., Bushy Park Plant, Charleston, SC 29411.

‡ Taken in part from the dissertation of X. Zhu which will be submitted to the Department of Chemistry in partial fulfillment of the Ph.D. degree.

10.1021/jp993430o CCC: $19.00
Published on Web 04/20/2000

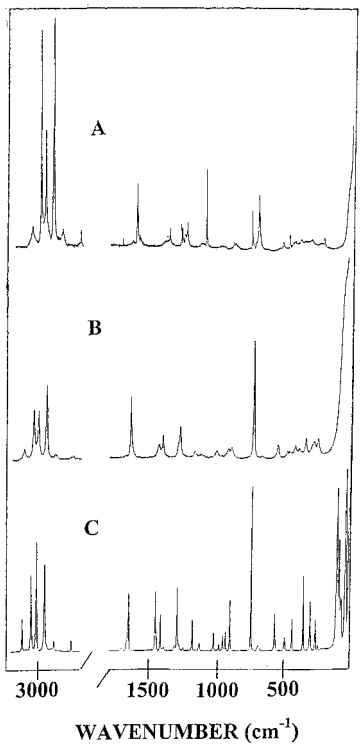

Figure 1. Raman spectra of 3,3-difluorobutene: (A) gas, (B) liquid, and (C) annealed solid (II).

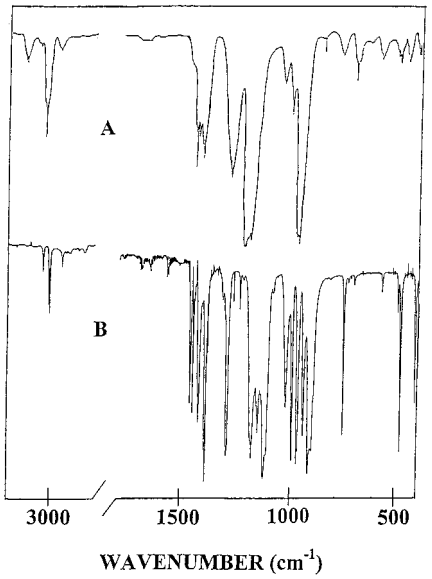

Figure 2. Mid-infrared spectra of 3,3-difluorobutene: (A) gas and (B) annealed solid (I).

a glass capillary which contained a spherical bulb on the end.[18] The spectrum of the annealed solid was obtained by condensing the sample on a blackened brass block, which was maintained in a cell fitted with quartz windows, cooled with boiling liquid nitrogen. The sample was annealed by raising the temperature of the sample to close to the melting point and then recooling the sample. This cycle was repeated until no further changes in the spectrum were noted. The representative Raman spectra of the gas, liquid, and solid are shown in Figure 1 and the reported frequencies for the observed lines which are listed in Table 1S (see Supporting Information paragraph at the end of the text) are expected to be accurate to ± 2 cm^{-1}.

The mid-infrared spectra (Figure 2) of the gas and the annealed solid from 3200 to 400 cm^{-1} were recorded with a

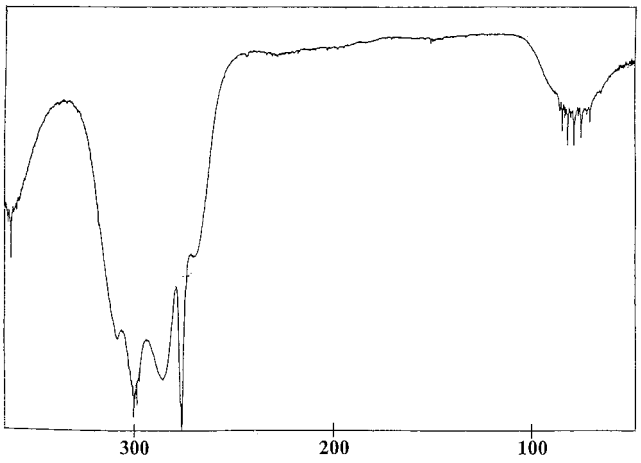

Figure 3. Far-infrared spectrum of gaseous 3,3-difluorobutene.

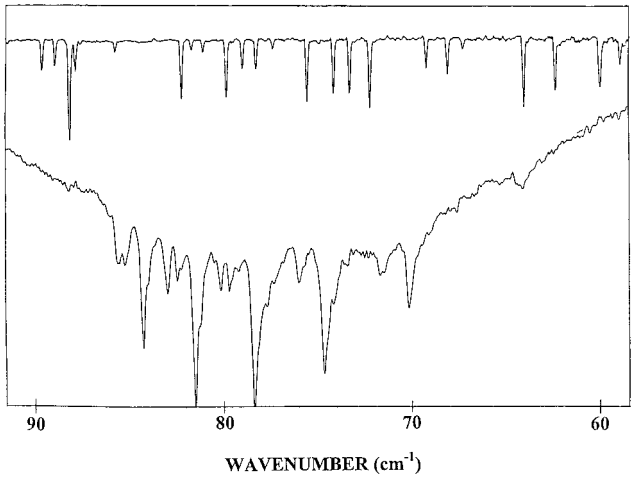

Figure 4. Far infrared spectrum of gaseous 3,3-difluorobutene from 92 to 58 cm^{-1}.

Digilab model FTS-14C Fourier transform spectrometer equipped with a Globar source, a Ge/KBr beam splitter and a triglycine sulfate (TGS) detector. The spectrum of the gas was obtained with the sample contained in a 12 cm cell equipped with CsI windows. Atmospheric water vapor was removed from the spectrometer housing by purging with dry nitrogen. For the solid, the spectrum was recorded by depositing a solid sample film onto a CsI substrate cooled by boiling liquid nitrogen and housed in a vacuum cell fitted with CsI windows. The sample was annealed until no further changes were observed in the spectrum.

The far infrared spectrum (Figure 3) of the gas from 380 to 80 cm^{-1}, from which the torsional transitions were measured (Figure 4), was recorded on a Nicolet model 200 SXV Fourier transform interferometer equipped with a vacuum bench, Globar source, liquid helium cooled Ge bolometer with a wedged sapphire filter and polyethylene windows. Traces of water were removed by passing the gas through activated 3 Å molecular sieves, using standard vacuum techniques. The gas was contained in a 1 m optical path cell with polyethylene windows. A 6.25 μm Mylar beam splitter was used to record the spectra at a resolution of 0.08 cm^{-1}. Typically, 256 scans were used for both the sample and reference, averaged and transformed with a boxcar truncation function to give a satisfactory signal-to-noise ratio.

The far infrared spectra (Figure 5) of the solids from 640 to 60 cm^{-1} were obtained with a Perkin-Elmer model 2000 Fourier transform spectrometer equipped with a far infrared grid beam splitter and a DTGS detector. The spectra were obtained by

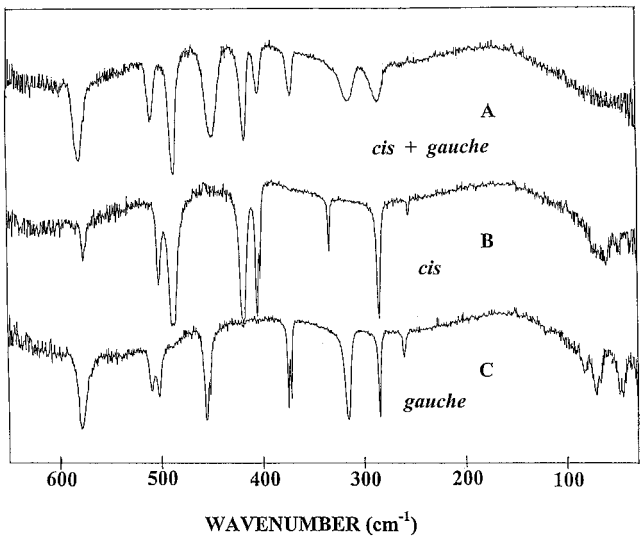

Figure 5. Far infrared spectrum of 3,3-difluorobutene: (A) amorphous solid, (B) annealed solid (I), and (C) annealed solid (II).

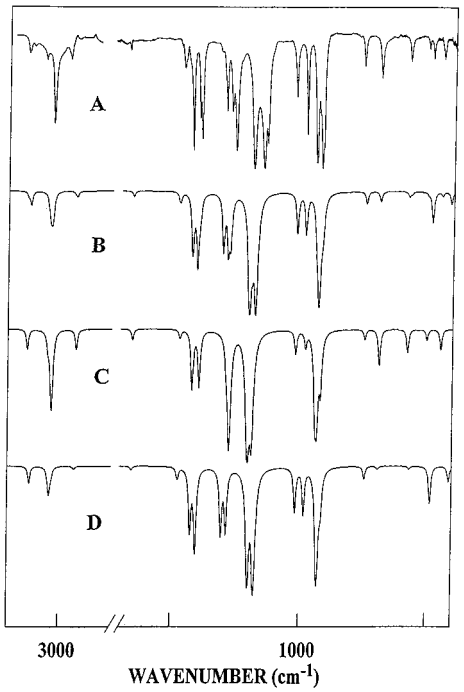

Figure 6. Mid-infrared spectra of 3,3-difluorobutene: (A) observed spectrum in xenon solution at −100 °C; (B) calculated spectrum of the mixture of both conformers; (C) calculated spectrum of the gauche conformer; and (D) calculated spectrum of the cis conformer.

condensing the sample on to a silicon plate held in a cell equipped with polyethylene windows and cooled with boiling liquid nitrogen. The sample was annealed until no further changes were observed in the spectrum. Two typical spectra of the annealed solids are shown in Figure 5, with the solid (Figure 5B) dominated by the cis conformer and the other (Figure 5C) by the gauche form.

The mid-infrared spectra (Figure 6) of the sample dissolved in liquefied xenon as a function of temperature were recorded on a Bruker model IFS-66 Fourier interferometer equipped with a Globar source, Ge/KBr beam splitter, and a DTGS detector. The spectra were recorded at variable temperatures ranging from −55 to −100 °C with 100 scans at a resolution of 1.0 cm^{-1}. The temperature studies in the liquefied noble gas were carried out in a specially designed cryostat cell, which is composed of a copper cell with a 4 cm path length and wedged silicon windows sealed to the cell with indium gaskets. The temperature was monitored by two Pt thermoresistors and the cell was cooled by boiling liquid nitrogen. The complete cell was connected to a pressure manifold to allow for the filling and evacuation of the cell. After the cell was cooled to the desired temperature, a small amount of sample was condensed into the cell. Next, the pressure manifold and the cell were pressurized with xenon, which immediately starts condensing in the cell, allowing the compound to dissolve.

Ab Initio Calculations

The geometry optimization of 3,3-difluorobutene was performed by the LCAO-MO-SCF restricted Hartree−Fock (RHF) calculations with the program Gaussian 94 using Gaussian-type basis sets.[19] The energy minimum with respect to the nuclear coordinates was obtained by the simultaneous relaxation of all geometric parameters using the gradient method of Pulay.[20] Calculations were also carried out with full electron correlation by the perturbation method[21] to second order, i.e., from MP2/6-31G(d) to MP2/6-311+G(2d,2p), and the predicted parameters are listed in Table 1. According to these ab initio calculations, the energy difference between the cis and gauche conformers varies from 378 to 58 cm^{-1}, respectively, from the MP2/6-31G(d), MP2/6-311G(d,p), MP2/6-311+G(d,p), and MP2/6-311+G(2d,2p) calculations, all favoring the gauche conformer as the more stable rotamer.

The optimized geometry was obtained from the MP2/6-311+G(d,p) calculation for the gauche conformer and then utilized to obtain a potential surface scan. In this potential surface scan only the torsional dihedral angle was allowed to vary in 10° increments from 0° to 180° (trans). The resulting potential function indicated an additional minimum at 0°, which corresponds to the cis conformer and the surface is given by the dashed line in Figure 7. Optimization at the cis and gauche minimum from the MP2/6-311+G(d,p) calculation gives energies of −355.028 259 and −355.028 833 hartree (1 hartree = 219 474 cm^{-1}), respectively, which are consistent with a more stable gauche conformer with the cis minimum lying 126 cm^{-1} higher in energy. Combined with optimization at torsional dihedral angles of 30°, 60°, 90°, 150°, and 180° utilizing MP2/6-311+G(d,p) calculations, this procedure leads to a more meaningful potential surface, and these data are illustrated by the solid line in Figure 7. Therefore, the theoretical cis to gauche and gauche to gauche barriers are 439 and 846 cm^{-1}, respectively.

The intramolecular harmonic force fields were calculated with the Gaussian 94 program[19] at the RHF/6-31G(d) and MP2/6-31G(d) levels. Internal coordinates were defined as shown in Figure 8, which were used to form the symmetry coordinates listed in Table 2S. The Cartesian coordinates obtained for the optimized geometry were used to calculate the B-matrix elements from the G-matrix program of Schachtschneider.[22] These B-matrix elements were use to convert the ab initio force fields in Cartesian coordinates to force fields in desired internal coordinates and the resulting force constants can be obtained from the authors. Briefly, if the internal coordinates R are defined in Cartesian coordinates X through the matrix relation $\mathbf{R} = \mathbf{B}x$, and the Cartesian force constants matrix F_x is obtained from the Gaussian ab initio frequency calculation, the force constant matrix $\mathbf{F}$ expressed in internal coordinates is related to F_x by $F_x = \mathbf{B}^T\mathbf{F}\mathbf{B}$, where T denotes the matrix operation of transposition. The inverse relation requires the result of diagonalization of the $(3N - 6) \times (3N - 6)$ matrix $\mathbf{B}\mathbf{B}^T$. If U is the

TABLE 1: Structural Parameters, Rotational Constants, Dipole Moments, and Total Energies for 3,3-Difluorobutene[a]

	RHF/6-31G(d)		MP2/6-31G(d)		MP2/6-311G(d,p)		MP2/6-311+G(d,p)		MP2/6-311+G(2d,2p)	
parameter[b]	cis	gauche	cis	gauche	cis	gauche	cis	gauche	cis	gauche
$r(C_1-C_2)$	1.315	1.315	1.335	1.334	1.336	1.335	1.337	1.337	1.331	1.331
$r(C_2-C_3)$	1.501	1.501	1.494	1.495	1.497	1.498	1.496	1.498	1.492	1.493
$r(C_3-C_4)$	1.508	1.510	1.503	1.506	1.505	1.508	1.504	1.507	1.499	1.502
$r(C_1-H_5)$	1.075	1.074	1.084	1.083	1.084	1.084	1.084	1.084	1.078	1.077
$r(C_1-H_6)$	1.075	1.075	1.084	1.084	1.084	1.084	1.084	1.084	1.080	1.077
$r(C_2-H_7)$	1.077	1.076	1.087	1.087	1.087	1.086	1.087	1.087	1.080	1.080
$r(C_3-F_8)$	1.356	1.355	1.385	1.384	1.375	1.375	1.380	1.380	1.380	1.381
$r(C_3-F_9)$	1.356	1.350	1.385	1.378	1.375	1.368	1.380	1.371	1.380	1.372
$r(C_4-H_{10})$	1.082	1.083	1.091	1.092	1.091	1.092	1.091	1.092	1.084	1.084
$r(C_4-H_{11})$	1.082	1.083	1.091	1.091	1.091	1.091	1.091	1.091	1.083	1.084
$r(C_4-H_{12})$	1.082	1.082	1.091	1.091	1.091	1.091	1.091	1.091	1.083	1.084
$\angle C_1C_2C_3$	126.0	124.3	125.0	123.3	125.2	123.6	124.8	123.8	124.6	123.8
$\angle C_2C_3C_4$	118.3	114.7	118.6	115.2	117.9	114.4	118.2	114.7	118.1	114.9
$\angle C_2C_1H_5$	122.8	121.9	122.4	121.4	122.0	121.0	122.1	121.2	121.9	121.0
$\angle H_6C_1C_2$	120.9	121.1	121.0	121.2	120.7	120.9	120.6	120.6	120.7	120.7
$\angle H_7C_2C_1$	120.9	121.3	121.2	121.6	121.2	121.6	121.3	121.5	121.1	121.3
$\angle F_8C_3C_2$	107.7	108.3	107.6	108.1	107.7	108.1	107.7	108.1	107.7	108.0
$\angle F_9C_3C_2$	107.7	110.2	107.6	110.1	107.7	110.3	107.7	110.4	107.7	110.3
$\angle H_{10}C_4C_3$	108.2	109.1	107.8	108.8	107.9	108.9	108.1	109.1	108.1	109.0
$\angle H_{11}C_4H_{10}$	108.9	109.0	109.2	109.3	109.3	109.4	109.2	109.4	109.2	109.4
$\angle H_{12}C_4H_{10}$	108.9	109.4	109.2	109.6	109.3	109.7	109.2	109.7	109.2	109.8
$\tau(C_4C_3C_2C_1)$	0.0	−113.8	0.0	−114.5	0.0	−113.9	0.0	−113.2	0.0	−113.0
$\tau(F_8C_3C_2C_4)$	−123.5	−121.1	−123.4	−121.3	−123.3	−121.0	−123.5	−121.2	−123.5	−121.1
$\tau(F_9C_3C_2C_4)$	123.5	123.1	123.4	123.0	123.3	122.9	123.5	123.3	123.5	123.3
$\tau(H_{10}C_4C_3C_2)$	180.0	182.3	180.0	181.8	180.0	182.4	180.0	182.1	180.0	182.8
$\tau(H_{11}C_4H_{10}C_3)$	−120.2	−120.4	−120.0	−120.1	−119.8	−120.1	−119.9	−120.1	−119.9	−120.0
$\tau(H_{12}C_4H_{10}C_3)$	120.2	120.3	120.0	120.0	119.8	119.9	119.9	119.9	119.9	120.0
$\lvert\mu_a\rvert$	2.011	0.946	2.209	1.014	2.282	1.040	2.448	1.114	2.363	1.040
$\lvert\mu_b\rvert$	1.419	0.815	1.483	0.547	1.582	0.743	1.732	0.735	1.649	0.689
$\lvert\mu_c\rvert$	0.000	1.942	0.000	2.186	0.000	2.225	0.000	2.404	0.000	2.317
$\lvert\mu_t\rvert$	2.462	2.309	2.661	2.471	2.777	2.566	2.999	2.749	2.881	2.631
A	5003	5153	4895	5038	4925	5055	4913	5042	4935	5062
B	2887	2853	2841	2838	2851	2839	2847	2829	2861	2847
C	2736	2832	2723	2798	2724	2807	2719	2798	2737	2811
$-(E+353)$	0.825403	0.827112	1.699883	1.701608	2.011218	2.012653	2.028259	2.028833	2.125545	2.125798
$\Delta E/cm^{-1}$	375		378		315		126		58	

[a] Bond lengths in Å, bond angles in degrees, rotational constants in MHz, dipole moments in debyes, and energies in hartrees. [b] For the definition of atom numbers, see Figure 8.

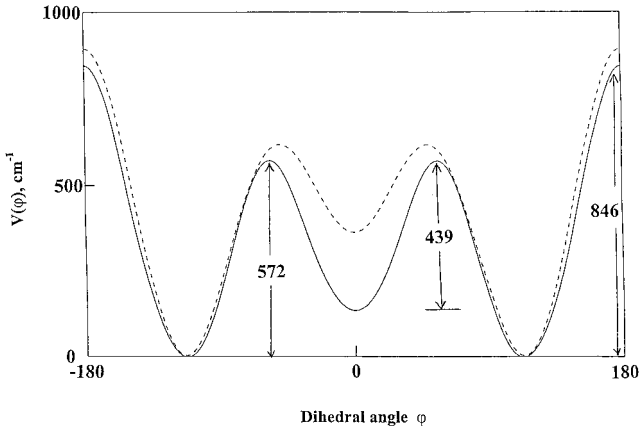

Figure 7. Potential function governing internal rotation of 3,3-difluorobutene as determined with the MP2/6-311+G** basis set. The potential surface given by the dashed line was obtained by allowing the torsional dihedral angle to vary by 10° increments while all other structural parameters were held fixed at the optimized value obtained for the gauche conformer. The potential surface given by the solid line was calculated by allowing for optimization at the gauche to gauche and gauche to cis transition states and at the gauche minimum by relaxation of all the geometric parameters.

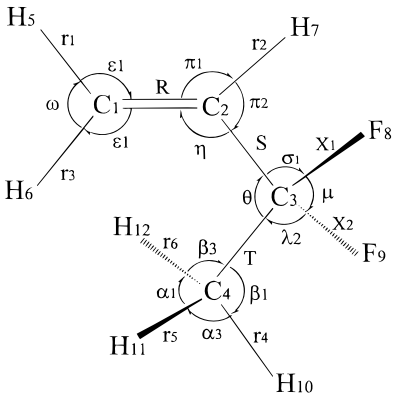

Figure 8. Internal coordinates for 3,3-difluorobutene.

orthogonal similarity transformation that diagonalizes $\mathbf{BB}^T$, and if Γ is the diagonal matrix of its nonzero eigenvalues, while Γ^{-1} is the inverse of Γ, then algebra shows that $\mathbf{F} = \mathbf{U}\Gamma^{-1}\mathbf{U}^T\mathbf{B}F_x\mathbf{B}^T\mathbf{U}\Gamma^{-1}\mathbf{U}^T$. These force fields were used to reproduce the ab initio vibrational frequencies without a scaling factor. Scaling factors of 0.88 for carbon−hydrogen stretching modes, 0.9 for the heavy atom stretching and carbon−hydrogen bending modes, and 1.0 for the heavy atom bending modes and asymmetric torsion along with the geometric averages for the off-diagonal elements were input along with the force fields into the perturbation program to obtain the "fixed scaled" force fields, vibrational frequencies, and potential energy distributions (PED). These data are listed in Tables 2 and 3.

To aid in the vibrational assignment, the theoretical infrared spectra of both the cis and gauche conformers were calculated as well as mixtures of the two conformers with various energy

TABLE 2: Observed and Calculated Frequencies and Potential Energy Distribution (PED) for Cis Conformer of 3,3-Difluorobutene

species	vib no.	fundamental	ab initio[a]	fixed scaled[b]	IR intensity[c]	Raman activity[d]	dp ratio	obsd[e]	PED[f]
A′	ν_1	$=CH_2$ antisym str	3321	3115	6.5	54.4	0.65	(3109)	$99S_1$
	ν_2	CH str	3245	3044	1.3	132.2	0.24	3040	$85S_2$, $13S_4$
	ν_3	CH_3 antisym str	3237	3036	6.0	43.8	0.19	3013	$99S_3$
	ν_4	$=CH_2$ sym str	3228	3028	2.5	70.8	0.72	3008	$86S_4$, $13S_2$
	ν_5	CH_3 sym str	3135	2941	1.2	87.0	0.31	2953	$100S_5$
	ν_6	C=C str	1743	1655	1.5	21.3	0.17	1661	$68S_6$, $14S_8$
	ν_7	CH_3 antisym deformn	1556	1477	1.6	5.1	0.57	1463	$80S_7$
	ν_8	$=CH_2$ scissors	1501	1424	31.7	12.8	0.66	1424	$69S_8$, $10S_7$
	ν_9	CH_3 sym deformn	1477	1404	49.6	3.6	0.43	1393	$72S_9$, $16S_{10}$
	ν_{10}	=C−C str	1359	1304	34.1	15.4	0.34	1295	$18S_{10}$, $22S_9$, $20S_{17}$, $16S_{15}$
	ν_{11}	=CH in-plane bend	1351	1285	31.9	1.3	0.54	1267	$48S_{11}$, $18S_6$, $11S_{13}$
	ν_{12}	CF_2 sym str	1250	1200	102.6	1.8	0.71	1179	$24S_{12}$, $20S_{14}$, $11S_{13}$, $10S_{19}$
	ν_{13}	$=CH_2$ wag	1070	1017	19.7	7.0	0.73	1022	$38S_{13}$, $17S_{11}$, $13S_{12}$, $12S_{15}$, $10S_{14}$
	ν_{14}	CH_3 sym rock	977	927	22.0	2.8	0.69	939	$43S_{14}$, $21S_{13}$, $15S_{12}$
	ν_{15}	$C-CH_3$ str	782	743	4.9	8.3	0.03	753	$36S_{15}$, $27S_{12}$, $25S_{10}$
	ν_{16}	CF_2 scissors	577	567	1.1	1.3	0.72	576	$36S_{16}$, $15S_{18}$, $15S_{19}$, $14S_{12}$
	ν_{17}	CF_2 wag	491	484	16.0	0.8	0.41	488	$68S_{17}$, $15S_{10}$
	ν_{18}	C=CC bend	416	411	6.1	2.5	0.47	418	$32S_{18}$, $46S_{16}$
	ν_{19}	C−C−C bend	279	277	2.6	1.2	0.54	284	$57S_{19}$, $36S_{18}$
A″	ν_{20}	CH_3 antisym str	3239	3039	6.1	40.4	0.75	3013	$100S_{20}$
	ν_{21}	CH_3 antisym deformn	1549	1473	3.6	15.1	0.75	1450	$87S_{21}$
	ν_{22}	CH_3 antisym rock	1230	1178	136.0	2.2	0.75	1151	$40S_{22}$, $33S_{24}$, $21S_{27}$
	ν_{23}	$=CH_2$ twist	1036	983	20.9	1.6	0.75	992	$62S_{23}$, $36S_{26}$
	ν_{24}	CF_2 antisym str	981	930	86.0	1.0	0.75	969	$51S_{24}$, $42S_{22}$
	ν_{25}	$=CH_2$ rock	965	915	14.5	5.0	0.75	913	$93S_{25}$
	ν_{26}	dCH out-of-plane bend	721	691	1.2	4.8	0.75	705	$40S_{26}$, $28S_{23}$, $15S_{27}$
	ν_{27}	CF_2 rock	396	392	1.1	1.3	0.75	404	$56S_{27}$, $24S_{28}$, $10S_{22}$
	ν_{28}	CF_2 twist	323	319	0.3	5.4	0.75	333	$60S_{28}$, $17S_{26}$, $14S_{27}$
	ν_{29}	CH_3 torsion	283	269	0.04	0.1	0.75	(284)	$98S_{29}$
	ν_{30}	antisym torsion	87	87	0.3	7.9	0.75	(76)f	$100S_{30}$

[a] Calculated values are obtained from the MP2/6-31G(d) calculations. [b] Calculated using scaling factors of 0.88 for C−H stretches, 0.9 for C−H bends and heavy atom stretches and 1.0 for heavy atom bends and asymmetric torsion. [c] Infrared intensities are in km/mol obtained from the MP2/6-31G(d) calculations. [d] Raman activities in Å^4/amu from the RHF/6-31G(d) calcualtions. [e] Frequencies are from the infrared spectrum of the solid (I) except those in parentheses, which are from the infrared spectrum of the gas. [f] Predicted from the overtone frequency of 150.37 cm^{-1}.

differences between them. The infrared intensities were calculated based on the dipole moment derivatives with respect to the Cartesian coordinates. The derivatives were taken from the ab initio calculations transformed to normal coordinates by

$$\left(\frac{\partial \mu_u}{\partial Q_i}\right) = \sum_j \left(\frac{\partial \mu_u}{\partial X_j}\right) L_{ij}$$

where Q_i is the ith normal coordinate, X_j is the jth Cartesian displacement coordinate, and L_{ij} is the transformation matrix between the Cartesian displacement coordinates and normal coordinates. The infrared intensities were then calculated by

$$I_i = \frac{N\pi}{3c^2}\left[\left(\frac{\partial \mu_x}{\partial Q_i}\right)^2 + \left(\frac{\partial \mu_y}{\partial Q_i}\right)^2 + \left(\frac{\partial \mu_z}{\partial Q_i}\right)^2\right]$$

In Figure 6D the predicted infrared spectrum of the more stable cis conformer is shown and Figure 6C that for the gauche conformer. The predicted infrared spectrum of the mixture is shown in Figure 6B with the enthalpy difference of 68 cm^{-1} (value from xenon solution) with the cis conformer the more stable rotamer. The experimental infrared spectrum of 3,3-difluorobutene dissolved in liquid xenon at −100 °C is also shown for comparison in Figure 6A. The agreement between the observed and calculated spectra is excellent and these data were very valuable for making the vibrational assignment.

The Raman spectra have also been predicted from the ab initio calculated results. The evaluation of Raman activity by using the analytical gradient methods has been developed.[23,24] The activity S_j can be expressed as

$$S_j = g_j(45\alpha_j^{\,2} + 7\beta_j^{\,2})$$

where g_j is the degeneracy of the vibrational mode j, α_j is the derivative of the isotropic polarizability, and β_j is that of the anisotropic polarizability. The Raman scattering cross sections, $\partial\sigma_j/\partial\Omega$, which are proportional to the Raman intensities, can be calculated from the scattering activities and the predicted wavenumbers for each normal mode using the relationship:[25,26]

$$\frac{\partial \sigma_j}{\partial \Omega} = \left(\frac{2^4\pi^4}{45}\right)\left(\frac{(\nu_0 - \nu_j)^4}{1 - \exp\left[\frac{-hc\nu_j}{kT}\right]}\right)\left(\frac{h}{8\pi^2 c\nu_j}\right) S_j$$

where ν_0 is the exciting wavenumber, ν_j is the vibrational wavenumber of the jth normal mode, and S_j is the corresponding Raman scattering activity. To obtain the polarized Raman scattering cross sections, the polarizabilities are incorporated into S_j by $S_j[(1 - \rho_j)/(1 + \rho_j)]$, where ρ_j is the depolarization ratio of the jth normal mode. The Raman scattering cross sections and calculated wavenumbers obtained from the standard Gaussian program were used together with a Lorentzian function to obtain the calculated spectra.

TABLE 3: Observed and Calculated Frequencies and Potential Energy Distribution (PED) for Gauche Conformer of 3,3-Difluorobutane

species	vib no.	fundamental	ab initio[a]	fixed scaled[b]	IR intensity[c]	Raman activity[d]	dp ratio	obsd[e]	PED
A′	ν_1	$=CH_2$ antisym str	3331	3125	7.9	52.8	0.73	3115	$99S_1$
	ν_2	CH str	3246	3045	6.0	118.4	0.20	3052	$71S_2$, $27S_4$
	ν_3	CH_3 antisym str	3229	3029	19.4	65.4	0.72	3011	$49S_3$, $33S_{20}$, $10S_4$
	ν_4	$=CH_2$ sym str	3231	3031	19.8	60.9	0.74	3011	$57S_4$, $22S_3$, $20S_2$
	ν_5	CH_3 sym str	3128	2935	8.2	107.9	0.02	2953	$100S_5$
	ν_6	C=C str	1742	1654	4.3	31.7	0.19	1655	$68S_6$, $13S_8$
	ν_7	CH_3 antisym deformn	1548	1470	2.0	14.0	0.73	1457	$86S_7$
	ν_8	$=CH_2$ scissors	1496	1421	29.0	9.2	0.39	1420	$73S_8$
	ν_9	CH_3 sym deformn	1469	1394	27.3	0.5	0.52	1388	$89S_9$
	ν_{10}	C−C str	1352	1288	9.5	20.2	0.38	1298	$13S_{10}$, $18S_{11}$, $18S_6$, $12S_{13}$, $11S_8$
	ν_{11}	=CH in-plane bend	1332	1276	107.3	0.4	0.57	1252	$40S_{11}$, $20S_6$, $13S_{13}$
	ν_{12}	CF_2 sym str	1254	1204	172.6	4.4	0.74	1186	$13S_{12}$, $38S_{15}$, $16S_{17}$
	ν_{13}	$=CH_2$ wag	1070	1019	9.5	4.5	0.74	1030	$45S_{13}$, $18S_{11}$, $16S_{22}$
	ν_{14}	CH_3 sym rock	990	940	52.8	1.3	0.73	962	$36S_{14}$, $19S_{12}$, $10S_{13}$
	ν_{15}	$C-CH_3$ str	784	745	3.9	7.2	0.05	758	$20S_{15}$, $32S_{12}$, $30S_{10}$
	ν_{16}	CF_2 scissors	507	501	4.2	1.5	0.44	509	$73S_{16}$
	ν_{17}	CF_2 wag	453	446	18.2	2.7	0.59	454	$35S_{17}$, $24S_{27}$
	ν_{18}	C=CC bend	292	290	0.6	1.1	0.68	283	$31S_{18}$, $23S_{19}$, $20S_{29}$, $10S_{27}$
	ν_{19}	C−C−C bend	310	307	1.8	4.1	0.74	322	$44S_{19}$, $15S_{28}$, $11S_{26}$
A″	ν_{20}	CH_3 antisym str	3233	3033	9.3	45.3	0.30	3016	$66S_{20}$, $29S_3$
	ν_{21}	CH_3 antisym deformn	1547	1468	1.5	15.0	0.75	1448	$91S_{21}$
	ν_{22}	CH_3 antisym rock	1239	1190	105.7	5.5	0.61	1133	$23S_{22}$, $22S_{24}$, $14S_{27}$
	ν_{23}	$=CH_2$ twist	1033	980	6.5	2.2	0.72	992	$63S_{23}$, $31S_{26}$
	ν_{24}	CF_2 antisym str	985	934	58.3	4.2	0.74	944	$45S_{24}$, $29S_{22}$, $12S_{14}$
	ν_{25}	$=CH_2$ rock	970	920	27.5	3.7	0.67	911	$97S_{25}$
	ν_{26}	=CH out-of-plane bend	716	688	15.4	4.7	0.70	708	$34S_{26}$, $21S_{23}$, $14S_{15}$, $10S_{17}$
	ν_{27}	CF_2 rock	588	577	9.4	2.8	0.40	582	$16S_{27}$, $23S_{17}$, $21S_{18}$
	ν_{28}	CF_2 twist	371	368	0.8	1.1	0.53	373	$56S_{28}$, $18S_{27}$
	ν_{29}	CH_3 torsion	259	248	0.1	0.2	0.68	(255)	$74S_{29}$
	ν_{30}	antisym torsion	94	93	0.4	8.1	0.75	(84)	$90S_{30}$

[a] Calculated values are obtained from the MP2/6-31G(d) calculations. [b] Calculated using scaling factors of 0.88 for C−H stretches, 0.9 for C−H bends and heavy atom stretches, and 1.0 for heavy atom bends and asymmetric torsion. [c] Infrared intensities are in km/mol obtained from the MP2/6-31G(d) calculations. [d] Raman activities in $Å^4$/amu from the RHF/6-31G(d) calculations. [e] Frequencies are from the infrared spectrum of the solid (II) except those in parentheses, which are from the infrared spectrum of the gas.

The predicted Raman spectra of the pure cis and gauche conformers are shown in Figure 9,D and C, respectively. In Figure 9B the mixture of the two conformers is shown with the experimentally determined ΔH value of 68 cm^{-1} with the cis conformer the more stable form. The experimental Raman spectrum of the liquid is shown in Figure 9A for comparison and the agreement is considered satisfactory. Again, these spectral data were useful for making the vibrational assignment.

Vibrational Assignments

The cis conformer of 3,3-difluorobutene has C_s symmetry and the fundamental vibrations span the irreducible representation: 19A′ + 11A″. From the reasonable set of structural parameters (Table 1), it can be shown that the *c*-principal axis is perpendicular to the symmetry plane for the cis conformer. Therefore, the out-of-plane modes are expected to give rise to C-type infrared band contours and will yield depolarized Raman lines in the spectrum of the liquid and probably not be observed in the Raman spectrum of the gas, whereas the in-plane modes should give rise to A, B, or A/B hybrid type contours. The gauche form has only the trivial C_1 symmetry, so the infrared band contours can be A, B, C, or any hybrid combination. Thus, the vibrational analysis is based on the experimental spectra and predicted wavenumbers from the ab initio calculations, infrared intensities, Raman activities and depolarization ratios, and infrared band contours.

It is clear that there are two kinds of crystal modifications by annealing the sample as shown in Figure 5. According to the ab initio calculations, the C=C−C bend and CF_2 rock for the cis conformer have been predicted at 411 and 392 cm^{-1} respectively. In the infrared spectrum of the amorphous solid, two bands were observed at 417 and 403 cm^{-1}, which are present (Figure 5B) in the infrared spectrum of solid (I) and absent (Figure 5C) in the infrared spectrum of solid (II). Similarly, the CF_2 rock and twist for the gauche conformer have been predicted to be at 446 and 368 cm^{-1}, respectively, and these modes are observed in the infrared spectrum of the amorphous sample as well as in the spectrum (Figure 5C) of solid (II). Therefore, the cis conformer is the only rotamer existing in solid (I), and the gauche conformer the only form in solid (II). Thus, we assigned all the observed bands in the infrared spectra of solids (I) and (II) to the cis and gauche conformers, respectively.

Carbon−Hydrogen Modes. The =C−H stretch has been predicted to have the second highest frequency with the expected wavenumber of 3044 cm^{-1}, so the peak in the infrared spectrum of the solid at 3040 cm^{-1} is assigned to this mode. In our previous study[3] of 1-butene, the $=CH_2$ symmetric stretch was assigned at 3008 cm^{-1} in the Raman spectrum of the gas. Thus, the peak at 3014 cm^{-1} in the Raman spectrum of the gas of 3,3-difluorobutene is assigned to the corresponding mode for the cis conformer. The $=CH_2$ antisymmetric stretch is expected to be the highest frequency fundamental and to have low infrared intensity so the weak band at 3109 cm^{-1} has been assigned to this mode. Since only the gauche conformer remains in solid

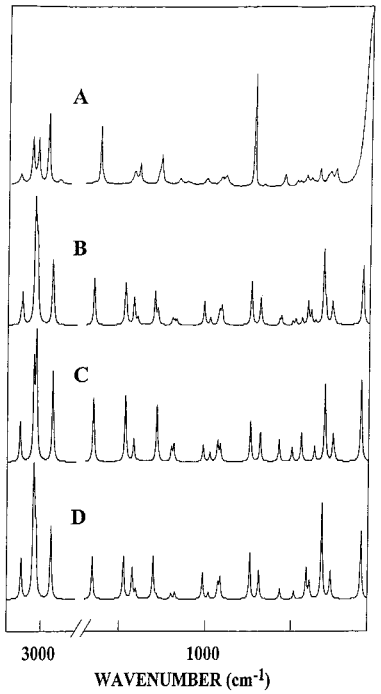

Figure 9. Raman spectra of 3,3-difluorobutene: (A) observed spectrum of the liquid; (B) calculated spectrum of the mixture of both conformers; (C) calculated spectrum of the gauche conformer; and (D) calculated spectrum of the cis conformer.

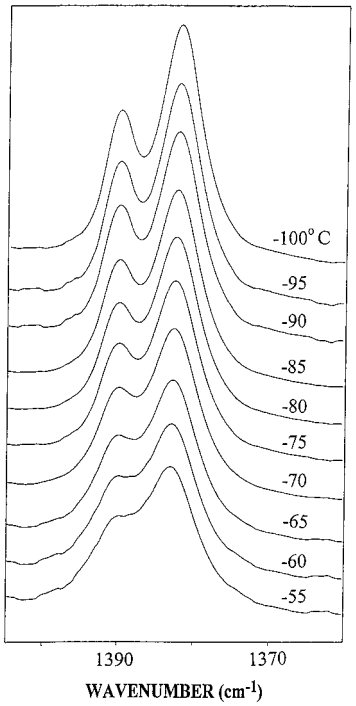

Figure 10. Temperature dependence of 1390 and 1382 cm^{-1} infrared bands of 3,3-difluorobutane in liquid xenon.

(II), all the bands in the Raman spectrum of solid (II) in this region have been assigned to this conformer.

It is reasonable to compare the assignments of the carbon−hydrogen bending modes for this difluoride molecule with the corresponding modes[3] of 1-butene. For the cis conformer of 1-butene, the $=CH_2$ scissors, wag, twist, and rock were assigned at 1426, 1071, 999, and 915 cm^{-1}, respectively, and in the infrared spectrum of 3,3-difluorobutene of solid (I), four sharp bands have been observed at 1424, 1022, 992, and 913 cm^{-1}. Thus, it is reasonable to assign these bands as the corresponding modes for the cis conformer of the corresponding difluoride molecule. These assignments are consistent with the predicted wavenumbers and infrared intensities from the ab initio calculations. The corresponding assignments can be made for the gauche conformer utilizing the spectral data from solid (II). The similar analysis for the assignments of the CH_3 stretching and bending modes for the cis and gauche conformers is relatively straightforward utilizing the data from solid (I) and solid (II), respectively, along with the ab initio predictions.

Skeletal Modes. From the infrared spectrum of solid (I), the CF_2 symmetric and antisymmetric stretching modes for the cis conformer have been assigned to two relatively intense bands at 1179 and 969 cm^{-1}. The two C−C stretches have been assigned to the bands at 1296 and 753 cm^{-1} mainly based on the ab initio calculations and predicted PED.

The most challenging assignments are those in the low-frequency region where the skeletal bending modes are found for the anti conformer of 2,2-difluorobutane,[27] where the CF_2 scissors, wag, rock, and twist have been assigned at 584, 517, 444, and 358 cm^{-1}, respectively. Because of the similarity of the bending modes of the CF_2 moiety between those of 2,2-difluorobutane and 3,3-difluorobutene, the sharp bands at 576, 488, 404, and 333 cm^{-1} in the infrared spectrum of solid (I) have been assigned to the corresponding modes for the cis conformer of the latter molecule. The corresponding modes for the gauche conformer are observed at 509, 454, 582, and 373 cm^{-1} in the infrared and/or Raman spectrum of solid (II), and the values are in excellent agreement with the predicted values of 501, 446, 577, and 368 cm^{-1} (Table 3), respectively. Some of these assignments were used in supporting the determination of which conformer remains in each of the solid phases. The other two skeletal modes excluding the asymmetric torsion, the C=C−C and C−C−C bends, are assigned at 418 and 284 cm^{-1}, respectively, from the infrared spectrum of the solid for the cis conformer and at 283 and 322 cm^{-1}, respectively, for the gauche conformer from the Raman spectrum of the solid. These modes are predicted quite well from the ab initio calculations.

The methyl torsions for the cis and gauche conformers of 3,3-difluorobutene are predicted to be at 269 and 248 cm^{-1}, respectively, both with low infrared intensities. This mode for the cis conformer gives rise to a C-type infrared contour, whereas from the ab initio predictions, the corresponding mode for the gauche rotamer should have an A/B hybrid infrared contour. In the far-infrared spectrum of the gas, a very weak Q-branch is observed at 255 cm^{-1} which has been assigned as the methyl torsion of the cis conformer, whereas a broad weak band at 242 cm^{-1} is assigned as the corresponding mode for the gauche rotamer.

Conformational Stability

The determination of the conformational stability is rather difficult since most of the fundamentals for each conformer are predicted to be near coincident. Nevertheless, as documented above, it is clear from the spectral data that two conformers are present in the fluid phases. The conformer pairs at 983/1148, 1390/1382 (Figure 10) and 1266/1250 cm^{-1} (Figure 11) with the first listed frequencies due to the cis conformer, were used to determine the enthalpy difference between the conformers. From these spectral data, it is obvious that the increase in the relative peak heights of the infrared bands assigned to the cis conformer as the temperature decreases confirms the stability of the cis form over the gauche rotamer in the xenon solution. In order to obtain the enthalpy difference, spectral data at 10

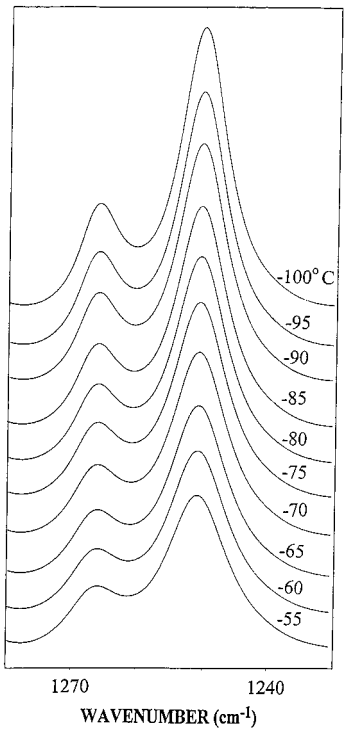

Figure 11. Temperature dependence of 1266 and 1250 cm^{-1} infrared bands of 3,3-difluorobutene in liquid xenon.

TABLE 4: Temperature and Intensity Ratios from Conformational 3,3-Difluorobutene

T (°C)	1000/T (K)	I_{1266}/I_{1250}	I_{983}/I_{1148}	I_{1390}/I_{1382}
−55	4.58	0.1547	0.1962	0.2813
−60	4.69	0.1541	0.1925	0.2837
−65	4.80	0.1544	0.1946	0.2876
−70	4.92	0.1583	0.1994	0.2882
−75	5.05	0.1610	0.2031	0.2961
−80	5.18	0.1608	0.2061	0.2985
−85	5.31	0.1596	0.2068	0.3065
−90	5.46	0.1638	0.2139	0.3050
−95	5.61	0.1722	0.2123	0.3108
−100	5.78	0.1719	0.2157	0.3161
ΔH^a (cm^{-1})		66 ± 8	68 ± 7	69 ± 4

[a] Average value is 68 ± 4 cm-1 (0.81 ± 0.05 kJ/mol) with the cis conformer the more stable rotamer.

different temperatures were obtained from these pairs of bands over the temperature range from −55 to −100 °C (Table 4). The intensities (areas under the peaks) of the conformer pairs were fit to the equation $-\ln K = (\Delta H/RT) - (\Delta S/R)$ where K is the intensity ratio (I_c/I_g) and it is assumed that ΔH is not a function of temperature. Using a least-squares fit, and from the slope of the line, an average ΔH value of 68 ± 4 cm^{-1} (0.81 ± 0.04 kJ/mol) was obtained from these three conformer pairs.

Asymmetric Torsion

The far-infrared spectrum of a gaseous molecule, which has an asymmetric internal rotor, can be a source of detailed information about the barriers to conformational interchange. The far-infrared spectrum of 3,3-difluorobutene is shown in Figures 3 and 4. In the spectral region of the asymmetric torsion, pronounced sharp Q-branches occur at 84.27, 81.55, 78.36, 74.69, and 70.10 cm^{-1}, with additional weaker Q-branches at 85.52, 82.93, 80.12, 75.96, and 71.67 cm^{-1}. The five pronounced Q transitions at 84.27, 81.55, 78.36, 74.69, and 70.10 cm^{-1} appear to form a reasonable series and have been assigned as the first five transitions of the torsional mode for the gauche conformer because of the degeneracy of two for the gauche conformer as well as the predicted higher infrared intensity of the gauche torsional mode (Tables 2 and 3) relative to the corresponding mode for the cis form. The weak Q-branch series beginning at 85.52 cm^{-1}, which fall to the low frequency, are probably due to the torsional transitions that arise from an excited mode of the C−C−C bending mode for the gauche conformer. Also, a number of sharp bands are observed in the far-infrared regions from 150 to 140 cm^{-1} at 150.37, 149.28, 148.30, 146.45, 145.18, and 144.38 cm^{-1} (Figure 12). In this region one might expect to observe the two quantum transitions of the asymmetric torsion of one of the conformers. The wavenumber for the first observed transition in the higher frequency series is too low for the overtone of the Q-branches at 84.27 and 81.55 cm^{-1}, and therefore, these overtones must be assigned to the torsional modes of the cis conformer where the 2 ← 0 transition is assigned at 150.37 cm^{-1}. Therefore, the more intense the bands at 148.30 and 145.18 cm^{-1} are assigned as the 3 ← 1 and 4 ← 2 overtones of the cis conformer and these three bands along with the five transitions for the gauche conformer will be used to obtain barriers for the conformational interchange.

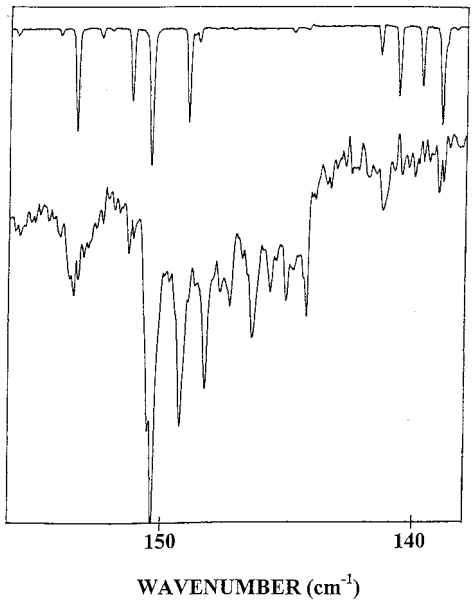

Figure 12. Far infrared spectrum of gaseous 3,3-difluorobutene from 156 to 138 cm^{-1}.

Discussion

In the present study of 3,3-difluorobutene, the cis conformer has been identified as the more stable conformer with an enthalpy difference of 68 ± 4 cm^{-1} from the xenon solution, which is a similar value to those of 3,3-difluoropropene[28] and 1-butene.[3] Although all the ab initio calculations predict the gauche conformer to be the more stable form, the experimental results are as reliable as the assignments on which they are based. This value of ΔH is expected to be similar to the value for the gas since the dipole moments and molecular sizes of the two conformers are predicted to be nearly the same.[29−33]

The MP2/6-311+G(d,p) ab initio calculations predict that the C_2-C_3 and C_3-C_4 bond distances are 0.003 and 0.004 Å longer, respectively, for the gauche conformer than the corresponding bonds for the cis rotamer. The C_3-F_9 bond distance for the gauche form is 0.009 Å shorter than the corresponding distance for the cis conformer. However, the corresponding force constants for these three bonds for the two conformers are only

slightly different which results in small differences in the vibrational frequencies between the two conformers for the motions associated with these bonds. Major differences in the structural parameters are also predicted for the CCC and CCF angles, with values of 3.5° larger and 2.7° smaller, respectively, for the cis conformer than those for the gauche conformer. Because of these differences, the bending force constant for the CCC angle increases by about 20% for the cis conformer, whereas the bending force constant for the CCF angle decreases by almost the same amount. These changes in the bending force constants result in larger differences in the vibrational frequencies for the modes associated with these angle bends. For example, the CF_2 scissors shifts from 576 cm^{-1} for the cis conformer to 509 cm^{-1} for the gauche form. For this reason, bending modes are much more indicative of the presence of conformers for these types of molecules than the bond stretching motions. Although a lot of the force constants between the two conformers have nearly the same values, there are still some significant frequency differences for the corresponding modes, especially for some of the bending motions. Many of these differences are due to the differences in the mixing of the molecular modes.

Two scaling factors of 0.88 and 0.9 have been used to obtain the predicted frequencies for the normal modes and the potential energy distributions (PED) from the MP2/6-31G(d) calculations. The scaled frequencies are in excellent agreement with the observed values with the average errors in the frequency predictions for all 30 normal modes of 12 and 10 cm^{-1} for the cis and gauche conformers, respectively. Thus, in the present study, multiple scaling factors are not warranted for predicting the frequencies of the fundamentals for aiding in the vibrational assignments for the normal modes for the two conformers.

The PEDs indicate there is extensive mixing of the fundamental vibrations for the two conformers, especially for the gauche conformer which has no symmetry. For example, for the gauche conformer, the band at 1298 cm^{-1} which is assigned as the C−C stretch is made up of five different contributions with none greater than 18%. Nevertheless, there are still a significant number of vibrations that are relatively pure for each of the conformers.

Utilizing the fundamental methyl torsional frequency for the gauche conformer, one can calculate the barrier to internal rotation. From a previous study[4] of 1-butene, the methyl torsional barriers were determined to be 1320 ± 57 and 1120 ± 63 cm^{-1} for the cis and gauche conformers, respectively. The corresponding values obtained from this study of 3,3-difluorobutene for the cis and gauche conformers are 1481 and 1339 cm^{-1}, respectively. There are two effects which significantly increase the methyl torsional barrier for 1-butene. These are the steric hindrance between the methyl group and the hydrogen atoms as well as the nonbonded attraction between the methyl group and the π system. If the CH_2 group were replaced by the CF_2 group, since the van der Waals radius of fluorine atom is larger than that of hydrogen atom, one might expect that the methyl torsional barrier of 3,3-difluorobutene would be higher than that of 1-butene, which is what was found from the experiment. The replacement of two hydrogen atoms by two fluorine atoms raises the ethane barrier by about 0.4 kcal/mol for 1,1-difluoroethane.[34] Therefore, the barriers of the CH_3 rotors for the cis and gauche conformers of 3,3-difluorobutene would be expected to be around 1460 and 1260 cm^{-1}, respectively, based on the earlier values obtained for the corresponding rotors of 1-butene, which are in good agreement with the determined values in the present study.

TABLE 5: Observed Asymmetric Torsional Transitions of 3,3-Difluorobutene

transition	obsd (cm^{-1})	calcd (cm^{-1})	Δ^a
gauche			
$1\mp \leftarrow 0\pm$	84.27	83.32	0.95
$2\pm \leftarrow 1\mp$	81.55	81.65	−0.10
$3\mp \leftarrow 2\pm$	78.36	79.27	−0.91
$4\pm \leftarrow 3\mp$	74.69	75.97	−1.28
$5\mp \leftarrow 4\pm$	70.10	71.12	−0.96
cis			
$2 \leftarrow 0$	150.37	151.02	−0.65
$3 \leftarrow 1$	148.30	149.07	−0.77
$4 \leftarrow 2$	145.18	145.31	−0.13

[a] Calculated using $F_0 = 1.567\,861$, $F_1 = 0.104\,143$, $F_2 = -0.010\,700$, $F_3 = 0.000\,389$, $F_4 = 0.000\,092$, $F_5 = -0.000\,003$ cm^{-1} and the potential constant values listed in Table 6.

Utilizing the frequencies of the asymmetric torsional transitions for the cis and gauche conformers, the experimental enthalpy difference between the rotamers, and the gauche dihedral angle the potential function governing the conformer interconversion can be determined. The torsional potential is represented by a Fourier cosine series in the internal rotation angle ϕ:

$$V(\phi) = \sum_{i=1}^{6}\left(\frac{V_i}{2}\right)(1 - \cos i\phi)$$

where ϕ and i are the torsional angle and foldness of the barrier, respectively. It is assumed that V_5 is relatively small and it is not included in the series. Initially, the potential parameters V_1, V_2, and V_3 were calculated from the input of the frequencies for the two torsional transitions, i.e., the gauche fundamental at 84.27 cm^{-1} and the overtone at 150.37 for the cis form, the ΔH value of 68 cm^{-1}, the gauche dihedral angle of 114.8°, and the internal rotation constant $F(\phi)$. The internal rotation constant also varies as a function of the internal rotation angle, and this is approximated by another Fourier series

$$F(\phi) = F_0 + \sum_{i=1}^{5} F_i \cos i\phi$$

The relaxation of the structural parameters, $B(\phi)$, during the internal rotation can be incorporated into the above equation by assuming them to be small periodic functions of the torsional angle of the general type

$$B(\phi) = a + b\cos\phi + c\sin\phi$$

The series approximating the internal rotation constants for 3,3-difluorobutene was determined by using structural parameters from the MP2/6-31G(d) ab initio calculations. As the calculations for the first three constants converged, additional torsional transitions of the gauche conformer, i.e., $\pm 2 \leftarrow \mp 1$, $\pm 3 \leftarrow \mp 2$, etc. were added along with the "hot bands" of the overtone for the cis conformer (Table 5). The V_4 and V_6 terms were added and the eight torsional transitions were fit to better than one wavenumber except for the $\pm 4 \leftarrow \mp 3$ transition of the gauche rotamer which differed by 1.28 cm^{-1} with relatively small values for the V_4 and V_6 terms. This potential gives a cis to gauche barrier of 557 cm^{-1} and a gauche to gauche barrier of 848 cm^{-1}. The final resulting values for the potential coefficients are listed in Table 6 and the potential function is shown in Figure 13.

For comparison purposes, we have predicted the potential parameters of the asymmetric torsion from the MP2/6-311+G-(d,p) calculations (Table 6). The V_1 and V_2 terms are signifi-

TABLE 6: Potential Constant Values (cm^{-1}) for the Asymmetric Torsion of 3,3-Difluorobutene and Barriers to Interconversion (cm^{-1})

	$CH_2CHCF_2CH_3$		CH_2CHCF_2H[b]		$CH_2CHCH_2CH_3$[c]	
potential const	exptl value[a]	MP2/6-311+G(d,p)	exptl value	MP2/6-311+G(d,p)	exptl value	MP2/DZ (2d,p)
V_1	284 ± 15	111	215 ± 16	372	−195 ± 43	−94
V_2	−164 ± 13	−278	−111 ± 17	−41	42 ± 20	−79
V_3	632 ± 7	602	633 ± 6	683	785 ± 14	707
V_4	−30 ± 5	22	54 ± 8	60	91 ± 11	88
V_5			−25 ± 4	−7		
V_6	−39 ± 3	−1	−12 ± 2	−12		
gauche dihedral angle	114.8 ± 0.3	113.2	113.0 ± 0.1	113.0	119.3	116.6
ΔH	68 ± 35	−126	82 ± 39	269	68	85
cis to gauche barrier	557	439	639	789	841	697
gauche to cis barrier	489	572	560	520	794	612
gauche to gauche barrier	848	846	744	778	637	682

[a] Calculated using the F numbers given in Table 7. [b] Data from ref 28. [c] Data from ref 35.

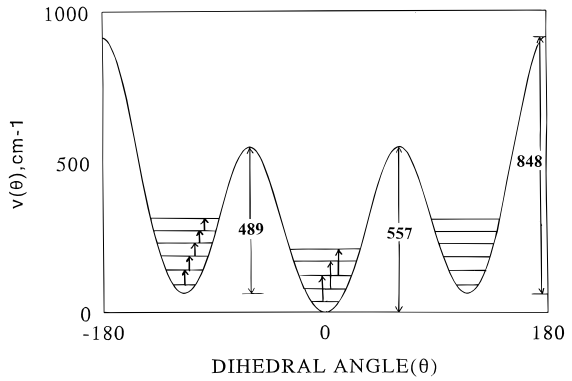

Figure 13. Asymmetric torsional potential function for 3,3-difluorobutene as determined from the spectral data. The torsional dihedral angle of 0° corresponds to the cis conformer.

cantly different from the experimental values since the ab initio calculations predict the gauche conformer to be more stable by 126 cm^{-1}, whereas the cis conformer was determined experimentally to be more stable by 68 cm^{-1} from the xenon solutions. Nevertheless, the V_3 term, which is the major term to the barrier to conformer interconversion is very close to the experimental value (predicted V_3 = 602 cm^{-1} versus 632 ± 7 cm^{-1} experimental value) obtained from the far-infrared data. The gauche to gauche barrier is predicted to be 846 cm^{-1} from the ab initio calculations, which is nearly the same as the value of 852 cm^{-1} determined from the experiment data.

It is of interest to compare the potential function governing the conformational interchange for 3,3-difluorobutene to those for 3,3-difluoropropene[28] and 1-butene.[3] As we reported[28] previously, for 3,3-difluoropropene, the potential parameters of V_1, V_2, and V_3 have values of 215 ± 16, −111 ± 17, and 633 ± 6 cm^{-1}, respectively, along with the cis to gauche and gauche to gauche barriers of 639 and 744 cm^{-1}, respectively. From this study of 3,3-difluorobutene, we obtained V_1 = 284 ± 15, V_2 = −164 ± 13, and V_3 = 632 ± 7 cm^{-1} with cis to gauche and gauche to gauche barriers of 549 and 852 cm^{-1}, respectively. Thus, the potential functions governing the conformational interchanges are very similar for these two molecules. These results indicate that the major effects for the torsional motion are the steric hindrance between the fluorine atoms and the hydrogen atom on the double bond, and the attractive force between the fluorine atoms and the double bond and the methyl group has little contribution to the potential function.

Because of the differences of the van der Waals radius and electronegativity between the fluorine atom and hydrogen atom, it might be expected that the potential parameters governing conformational interchange would be different between those for 3,3-difluorobutene and the corresponding potential for 1-butene. From a recent study of 1-butene,[35] the potential constants have been determined to be V_1 = −195 ± 43, V_2 = 42 ± 20, and V_3 = 785 ± 14 cm^{-1}, with the cis to gauche and gauche to gauche barriers of 841 and 637 cm^{-1}, respectively. Since the gauche dihedral angle for 1-butene is significantly different than those for $CH_2CHCF_2CH_3$ and CH_2CHCF_2H, the V_1 and V_2 terms are quite different for 1-butene. However, the V_3 term is only about 150 cm^{-1} larger than those for the other two molecules, but the cis to gauche barrier is larger than the gauche to gauche barrier for 1-butene as expected on steric predictions. Nevertheless, comparable potential functions are obtained for all three of these molecules.

The experimental study reported herein indicates evidence of at least two crystal modifications for 3,3-difluorobutene, solid (I) containing the cis conformer which appears first with annealing, and solid (II) the gauche rotamer. This is relatively unusual since the crystallization depends mainly on the packing of the molecules. Nevertheless, the fact that the dipole moment of the cis conformer is predicted to be only slightly larger than that of the gauche rotamer and the enthalpy difference is very small probably contributes to the presence of the two different crystals. It should be noted that it has not been possible[3,4] to crystallize 1-butene since the amorphous solid contains both conformers and repeated annealing does not change the conformer ratio. On the basis of the observed infrared band splittings for the two crystalline forms, there appears to be at least two molecules per primitive cell for both crystals. Therefore, the conversion of the crystal modifications of 3,3-difluorobutene from solid (I) to solid (II) indicates that the gauche conformer is favored by the crystal packing.

Acknowledgment. J.R.D. acknowledges the University of Kansas City Trustees for a Faculty Fellowship award for partial financial support of this research.

Supporting Information Available: Observed infrared and Raman wavenumbers (cm^{-1}) for 3,3-difluorobutene (Table 1S); symmetry coordinates for 3,3-difluorobutene (Table 2S). This material is available free of charge via the Internet at http://pubs.acs.org.

References and Notes

(1) Sheppard, N. *J. Chem. Phys.* **1949**, *17*, 74.
(2) Harrah, L. A.; Mayo, D. W. *J. Chem. Phys.* **1960**, *33*, 298.
(3) Durig, J. R.; Compton, D. A. C. *J. Phys. Chem.* **1980**, *84*, 773.
(4) Gallinella, E.; Cadiol, B. *Vibr. Spectrosc.* **1997**, *13*, 163.
(5) Bothnerby, A. A.; Naar-Colin, C. *J. Am. Chem. Soc.* **1961**, *83*, 231.
(6) Bothnerby, A. A.; Naar-Colin, C.; Gunther, H. *J. Am. Chem. Soc.* **1962**, *84*, 2748.

(7) Karabutsos, G. J.; Teller, R. A. *Tetrahedron* **1968**, *24*, 3923.
(8) Woller, P. W.; Garbisch, Jr., E. W. *J. Org. Chem.* **1972**, *37*, 428.
(9) Kondo, S.; Hirota, E.; Morino, Y. *J. Mol. Spectrosc.* **1968**, *28*, 4719.
(10) Durig, J. R.; Nanaie, H.; Guirgis, G. A. *J. Raman Spectrosc.* **1991**, *22*, 155.
(11) Durig, J. R.; Godbey, S. E.; Sullivan, J. F. *J. Chem. Phys.* **1984**, *80*, 5983.
(12) Sullivan, J. F.; Wang, A.; Durig, J. R.; Godbey, S. E. *Spectrochim. Acta* **1993**, *49A*, 1889.
(13) Durig, J. R.; Compton, A. C. *J. Phys. Chem.* **1980**, *84*, 773.
(14) Guirgis, G. A.; Nashed, Y. E.; Klaeboe, P.; Aleksa, V.; Durig, J. R. *Struct. Chem*. **1999**, *10*, 1.
(15) Guirgis, G. A.; Nashed, Y. E.; Gounev, T. K.; Durig, J. R. *Struct. Chem.* **1998**, *9*, 265.
(16) van der Veken, B. J.; Herrebout, W. A.; Durig, D. T.; Zhao, W.; Durig, J. R. *J. Phys. Chem.* **1999**, *103*, 1976.
(17) van der Veken, B. J.; Herrebout, W. A.; Durig, D. T.; Durig, J. R. *J. Phys. Chem.* **1999**, *103*, 6142.
(18) Furic, K.; Durig, J. R. *J. R. Appl. Spectrosc*. **1988**, *42*, 175.
(19) Frisch, M. J.; Trucks, G. W.; Schlegel, H. B.; Gill, P. M. W.; Johnson, B. G.; Robb, M. A.; Cheeseman, J. R.; Keith, T. A.; Petersson, G. A.; Montgomery, J. A.; Raghavachari, K.; Al-Laham, M. A.; Zakrzewski, V. G.; Ortiz, J. V.; Foresman, J. B.; Cioslowski, J.; Stefanov, B. B.; Nanayakkara, A.; Challacombe, M.; Peng, C. Y.; Ayala, P. Y.; Chen, W.; Wong, M. W.; Andres, J. L.; Replogle, E. S.; Gomperts, R.; Martin, R. L.; Fox, D. J.; Binkley, J. S.; Defrees, D. J.; Baker, J.; Stewart, J. P.; Head-Gordon, M.; Gonzalez, C.; Pople, J. A. *Gaussian 94*, Revision B.3; Gaussian Inc.: Pittsburgh, PA, 1995.
(20) Pulay, P. *Mol. Phys*. **1969**, *17*, 197.
(21) Moller, C.; Plesset, M. S. *Phys. Rev.* **1934**, *46*, 618.
(22) Schachtschneider, J. H. *Vibrational Analysis of Polyatomic Molecules;* Parts V and VI, Technical Report Nos. 231 and 57; Shell Development Co.: Houston, TX, 1964 and 1965.
(23) Frisch, M. J.; Yamaguchi, Y.; Gaw, J. F.; Schaefer III, H. F.; Binkley, J. S. *J. Chem. Phys*. **1986**, *84*, 531.
(24) Amos, R. D. *Chem. Phys. Lett*. **1986**, *124*, 376.
(25) Polavarapu, P. L. *J. Phys. Chem*. **1990**, *94*, 8106.
(26) Chantry, G. W. In *The Raman Effect*; Anderson, A., Ed.; Marcel Dekker Inc.: New York, 1971; Vol. 1, Chapter 2.
(27) Durig, J. R.; Yu, Z.; Guirgis, G. A. *J. Mol. Struct.* **1999**, *509*, 115.
(28) Durig, J. R.; Yu, Z.; Guirgis, G. A. *J. Phys. Chem*. **2000**, *104*, 741.
(29) Bulanin, M. O. *J. Mol. Struct.* **1973**, *19*, 59.
(30) Bulanin, M. O. *J. Mol. Struct.* **1995**, *347*, 73.
(31) van der Veken, B. J.; DeMunck, F. R. *J. Chem. Phys*. **1992**, *97*, 3060.
(32) Herrebout, W. A.; van der Veken, B. J. *J. Phys. Chem*. **1996**, *100*, 9671.
(33) Herrebout, W. A.; van der Veken, B. J.; Wang, A.; Durig, J. R. *J. Phys. Chem*. **1995**, *99*, 578.
(34) Fateley, W. G.; Miller, F. A. *Spectrochim. Acta* **1961**, *17*, 857.
(35) Bell, S.; Drew, B. R.; Guirgis, G. A.; Durig, J. R. *J. Mol. Struct.*, in press.